FACTA UNIVERSITATIS
Series: **Mechanical Engineering**
https://doi.org/10.22190/FUME230605039C

Original scientific paper

STUDY OF FRICTION COMPENSATION MODEL FOR MOBILE ROBOT'S JOINTS

Yanjie Cao, Norzalilah Mohamad Nor, Zahurin Samad

School of Mechanical Engineering, Universiti Sains Malaysia (USM), Penang, Malaysia

Abstract. *Frictional forces inside the joints of mobile robots hurt robot operation's stability and positioning accuracy. Therefore, establishing a suitable friction force compensation model has been a hot research topic in robotics. To explore the robot joint friction compensation model, three friction compensation models: linear, nonlinear, and neural network models, are developed in this paper. Based on the deep learning algorithm for three models at low speed, high speed, acceleration, and uniform speed training test, respectively results have been obtained. The test results show that the best friction compensation effect comes from combining neural network models in acceleration and a consistent speed state way. The friction compensation model trained this way yielded superior results to the other combinations tested. Finally, using the method, a friction compensation model trained by adding a neural network to the feedforward control torque was tested on a four-wheeled mobile robot platform. The test results show that the relative error of the torque caused by the friction of each joint is reduced by 15%-75% in 8 groups of tests, which indicates that our friction compensation method has a positive effect on improving the accuracy of the joint torque.*

Key words: *Deep Learning, Mobile robot joint, Friction compensation, Neural network*

1. INTRODUCTION

The presence of friction, especially nonlinear friction, can cause tracking errors, hysteretic motion, and limit-loop oscillations in industrial robots during low-speed, high-precision operation, affecting the smoothness of robot motion and reducing control accuracy [1]. Therefore, to improve the motion accuracy of mobile robots, it is necessary to study and analyze the frictional forces generated by the joints during industrial robot operation and implement compensation. The research on the analysis and settlement of frictional forces of industrial robot joints has become a hot research subject in the field of

Received: June 05, 2023 / Accepted October 23, 2023
Corresponding author: **Yanjie Cao**
School of Mechanical Engineering, Universiti Sains Malaysia (USM), 14300 Nibong Tebal, Penang, Malaysia
E-mail: caoyanjie@student.usm.my

the industrial robot [2], which has significant application value for improving the operation precision of industrial robot operation and overall performance.

A friction phenomenon between the joints of industrial robots is more complex, both sliding friction and rolling friction. Establishing a suitable friction model is the mainstream approach in current academia. Some empirical friction models have been proposed to compensate for the friction of robot joints. According to whether differential equations can describe the friction phenomena, there are static and dynamic friction models [3].

In the past, the linear and nonlinear viscous friction models appeared and were often used together with the Coulomb friction model, giving the Coulomb+Viscous model [4], on which Virgala et al. [5] introduced static friction to obtain the static friction + Coulomb + Viscous friction model. The common point in the above classical friction models is that the linear relationship between velocity and sliding friction and the interconversion between dynamic and static friction is carried out discretely. Richard et al. [6] proposed an exponential model to describe the phenomenon in 2007, which was later compensated by Nikfar et al. [7], an improved Stribeck friction model, in which the speed dependence of friction force was added. Keck et al. [8] studied the elastoplastic friction model parameter identification process, whereby a friction compensator was developed to estimate the state of the elastoplastic friction model. Beerens et al. [9] proposed a reset integrator control strategy to achieve robust global asymptotic stability for set points with unknown static friction. Marek Wojtyra [10] discussed the joint friction of a multi-body system with a closed-loop kinematic chain and solved the issue of uniqueness and high parameter sensitivity of the kinematic equation in a static friction zone.

Although the static friction force compensation model has the characteristics of a simple mathematical model structure and easy identification of parameters, it has a limited effect on improving the system performance.

Therefore, researchers have studied the dynamic friction model. Lampaert et al. [11] designed a dynamic friction model suitable for control purposes, which predicts the Stribeck effect and properties such as friction hysteresis, transition behavior, and disengagement forces. Xu et al. [12] proposed a friction compensation strategy based on robust adaptive control (ARC), which can guarantee the transient performance and final tracking accuracy of the mechanism in nonlinear dynamic friction scenarios. Joanna et al. [13] proposed a method to identify LuGre kinetic friction parameters that can significantly reduce trajectory tracking errors. The scholar Swevers [14] proposed the Leuven model to describe the hysteresis phenomenon more adequately, which is more accurate than the LuGre model, but recognizing the parameters of the model is more complicated. In addition, Lee et al. [15] proposed a new dynamic friction compensation technique that utilizes a PD control system and observer-based self-adaptive evaluation of friction to enhance the performance of tracking for motion control effectively. Maged et al. [16] proposed a physically motivated friction model that can be integrated quickly and smoothly into classic dynamic friction models such as LuGre and GMS. Piasek et al. [17] designed a method to identify LuGre's static and dynamic friction parameters and proved by experiments that the compensation of the dynamic friction model dramatically reduces the trajectory tracking error. Isaac et al. [18] designed the IDA-PBC friction compensation method of the LuGre model integrated to enhance the controller performance of the underactuated mechanical system at low speed. These have been meaningful explorations, but the dynamic friction compensation model in practical applications is still complex and challenging to identify parameters.

In recent years, some scholars have started using neural networks to study friction compensation. Ciliz et al. [19] proposed a friction compensation strategy based on the Coulomb and viscosity models, applying a neural network to predict the magnitude of friction. Doan et al. [20] disclosed a self-adaptation control system for robot operation using artificial neural networks for error compensation, which can compensate for unmodeled friction parts. Grami et al. [21] applied a neural network algorithm model to estimate the friction inside the robot joint and realized the estimated friction in the actual friction compensation. In addition, Yen et al. [22] designed a robust self-adaptable control approach with a fuzzy wavelet neural network system, which can reduce friction, external disturbance error and parameter variation and achieve a better control effect. Ali et al. [23] designed a control algorithm that combines FIT-SMC, RED and FFNN estimators, making the model-based friction compensation of the multi-degree-of-freedom robot system effective. Similarly, Wei et al. [24] disclosed an adaptive RBF neural network algorithm, which can reduce the influence of nonlinear and uncertain parts in the system on performance. Experimental results show that the jitter problem inherent to the sliding mode controller is also suppressed.

Because of the beneficial effects of deep learning algorithms in dealing with nonlinear and uncertain friction compensation, we decided to explore and study robot joint friction compensation in this direction. We establish linear, nonlinear, and neural network models and use deep learning algorithms to train them in four states: high speed, low speed, acceleration, and uniform speed. The conclusion shows that the neural network model has the best training effect under acceleration and consistent pace and is more suitable for robot joint friction compensation. The deep learning process we study allows automatic friction compensation to be applied at each mobile robot joint to obtain the best and most personalized friction compensation, which has practical value and improved accuracy.

The rest of this paper has the following arrangement: Section 2 describes the friction compensation modeling method, and the Scheme design, data collection, and data division are included. Section 3 presents the experiments and discussions. Section 4 shows the conclusions and future works.

2. FRICTION COMPENSATION MODELING

2.1 Program Design

The size of the friction in the robot joint is related to the structure, speed, load torque, lubrication conditions, and temperature of the robot joint. Nevmerzhitskiy et al. [25] disclosed the effect of temperature on friction. Bittencourt et al. [26] showed that the load significantly influences the friction model. Raviola, Andrea et al. [27] designed a mathematical model that can identify the dynamic parameters of the manipulator. Experiments show that this model reduces the error of the estimated joint torque of the robot.

The nonlinear frictional forces corresponding to this friction phenomenon are generated on the mobile robot's body, but direct measurement cannot obtain the corresponding frictional moment values. Therefore, the first task is to simplify the mobile robot dynamics model to get the importance of the friction moments of the robot's joints. The mathematical expression of the robot's dynamics model is shown in Fig. 1. The parameters involved are shown in Table 1.

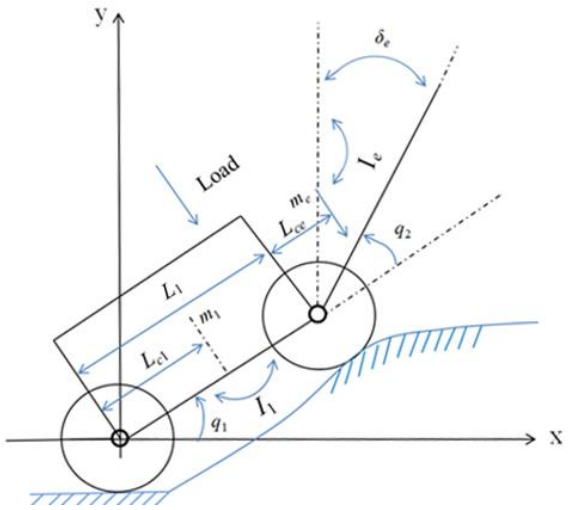

Fig. 1 Wheel of Mobile robot motion model

Table 1 Motion model parameters

Parameters	Description
m_1	Equivalent mass of the first rod
m_e	Equivalent mass of the second rod and payload
L_1	Length of first rod (wheel distance)
L_{c1}	Distance to the center of the first rod equivalent mass (wheel distance)
L_{ce}	Distance to the center of the second rod equivalent mass
I_1	Equivalent moment of inertia of the first rod
I_e	Equivalent moment of inertia of the second rod
q_1	Angle between the first rod and the horizontal axis
q_2	Angle between the first rod and second rod
δ_e	Angle between the second rod and the vertical axis

The kinetic model relates to the friction compensation term F as shown in Eq. (1).

$$M(q)\ddot{q}+C(q,\dot{q})\dot{q}+G(q)+F(\dot{q})=\tau \tag{1}$$

where $q \in R^n$ is the desired coordinates of the robot in space, $\dot{q} \in R^n$ is the joint angular velocity, $\ddot{q} \in R^n$ is the angular acceleration of the joint, $M(q) \in R^{n \times n}$ is the robot's positive definite inertia matrix, $C(q,\dot{q}) \in R^{n \times n}$ is the Coriolis force matrix, $G(q) \in R^n$ is the gravitational vector, $F(\dot{q}) \in R^n$ is the robot joint friction, $\tau \in R^n$ is the joint input torque, and n represents the nth robot joint.

$$M(q)=\begin{pmatrix} \alpha+2\varepsilon\cos(q_2)+2\eta\sin(q_2) & \beta+\varepsilon\cos(q_2)+2\eta\sin(q_2) \\ \beta+\varepsilon\cos(q_2)+\eta\sin(q_2) & \beta \end{pmatrix} \tag{2}$$

$$C(q,\dot{q}) = \begin{pmatrix} (-2\varepsilon\sin(q_2)+2\eta\cos(q_2))\dot{q}_2 & (-\varepsilon\sin(q_2)+\eta\cos(q_2))\dot{q}_2 \\ (\varepsilon\sin(q_2)-\eta\cos(q_2))\dot{q}_1 & 0 \end{pmatrix} \tag{3}$$

$$G(q) = \begin{pmatrix} \varepsilon e2\cos(q_1+q_2)+\eta e2\sin(q_1+q_2)+(\alpha-\beta+e1)e2\cos(q_1) \\ \varepsilon e2\cos(q_1+q_2)+\eta e2\sin(q_1+q_2) \end{pmatrix} \tag{4}$$

where: $\alpha = I_1 + m_1 l_{c1}^2 + I_e + m_e l_{ce}^2 + m_e l_1^2$, $\beta = I_e + m_e l_c e^2$, $\varepsilon = m_e I_1 l_{ce}\cos\delta_e$, $\eta = m_e I_1 l_{ce}\sin\delta_e$, $e_1 = m_1 I_1 l_{cl} - I_1 - m_1 l_{m1}{}^2$, $e_2 = g / l_1$

The actual compensation for the various frictional forces in the robot joints during motion is done in the following manner (Fig. 2).

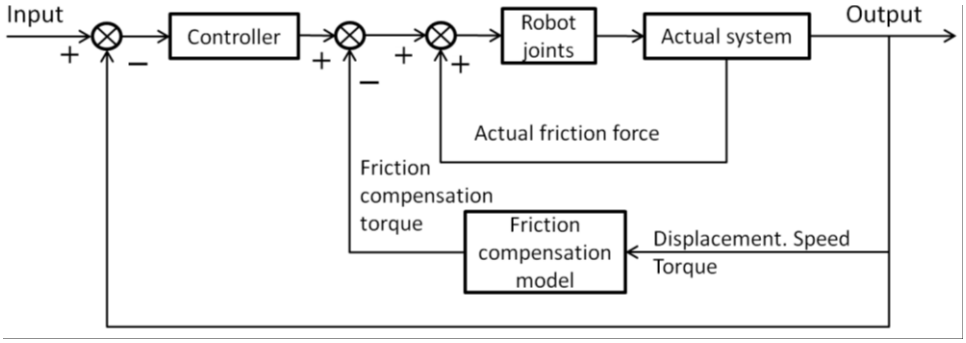

Fig. 2 Friction compensation closed-loop control system structure

Because the friction force includes static friction, sliding friction, viscous friction, etc., the influencing factors are relatively complex and have non-linear characteristics. Our study uses three different models to model the frictional forces: 1) a traditional linear mathematical model, 2) a nonlinear mathematical model and 3) a deep learning Neural Network model.

2.2 Building the Model

Three models are investigated separately: 1) linear model, 2) nonlinear model, and 3) Neural Network model.

2.2.1 Traditional Friction Model: Linear Model

The essence of the linear compensation model is to use the form of setting linear coefficients to realize the friction compensation by using the coefficients c_o-c_4:

$$F = c_0 + c_1 \cdot v + c_2 \cdot \tau + c_3 \cdot T + c_4 \cdot q \tag{5}$$

where, F is the overall friction force, v is velocity, τ the torque, T is the temperature, q is the position term and c_o-c_4 are the constant (c_o takes the value 1.0, c_1 the value 1.2, c_2 the value 3.6, c_3 is 1.0, and c_4 takes the value 4.3).

2.2.2 Traditional Friction Model: Nonlinear Model

The conventional friction model can also be expressed in a nonlinear form as:

$$F = \sqrt{2e}\left(F_{brk} - F_c\right)\cdot\exp\left(-\left(\frac{v}{v_{st}}\right)^2\right)\cdot\frac{v}{v_{st}} + F_c\cdot\tanh\left(\frac{v}{v_{coul}}\right) + fv \tag{6}$$

where:

$$v_{st} = v_{brk}\sqrt{2} \tag{7}$$

$$v_{coul} = \frac{v_{brk}}{10} \tag{8}$$

Here, F is the overall friction force, F_c the Coulomb force, F_{brk} the maximum static friction, v_{brk} is the maximum static friction velocity, v_{St} the viscous friction velocity threshold, v_{coul} the Coulomb velocity threshold, v the relative velocity and fv is the viscosity coefficient.

2.2.3 Neural Network Model

Because the robot joint friction has significant nonlinear characteristics, we use a neural network model to solve the problem of friction compensation. The input feature quantities of the neural network model are torque, velocity, position, temperature, etc. Its output is the friction force. The weights in the network are adjusted according to the loss function of its error magnitude to make the model converge.

The feedforward neural network has a simple structure and is widely used. It can approximate any continuous function and square integrable function with any precision. Moreover, it can accurately implement any finite training sample set and obtain complex nonlinear processing capabilities. We designed a feed-forward neural network in which information is input from the input layer, and neurons in each layer receive inputs from the previous layer and output to the next layer up to the output layer. The constructed neural network model includes several stacked structural modules, and the number of modules can be changed through the programming API. Each stacking structure module consists of a batch normalization layer, a fully connected layer, and an activation layer (Fig. 3).

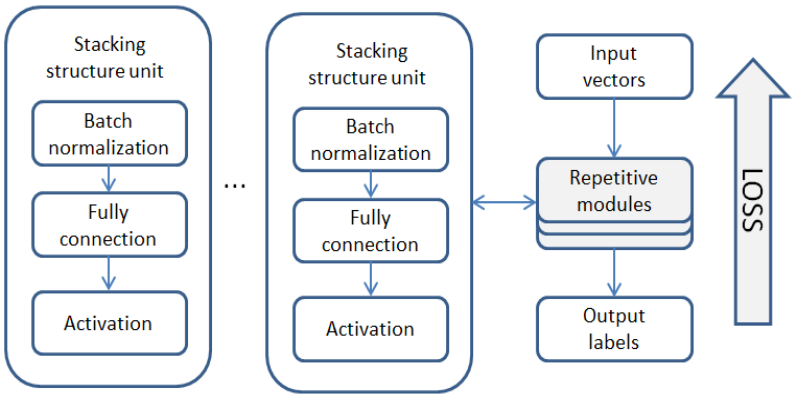

Fig. 3 Deep learning algorithm model

A neural network consists of an input, implicit, and output layer. The number of hidden layers and neurons per layer is adjustable. It is worth noting that the number of different layers and the number of neurons per layer significantly impact the model performance. Thoma et al. [28] showed that feedforward neural networks with two hidden layers have better generalization ability than feedforward neural networks with one hidden layer.

Too few neurons in the hidden layer can lead to underfitting, and conversely, too many neurons in the hidden layer may lead to overfitting. For the friction compensation model, the robot's friction force is a nonlinear function related to various influencing factors. The five input features of the friction compensation algorithm model are the position, velocity, theoretical torque, actual torque, and temperature of each wheel joint. The output is the friction force of each joint. Considering the model's fitting ability and convergence difficulty, the number of implied layers is three, and the number of neurons per layer is determined to be 5 (Fig. 4).

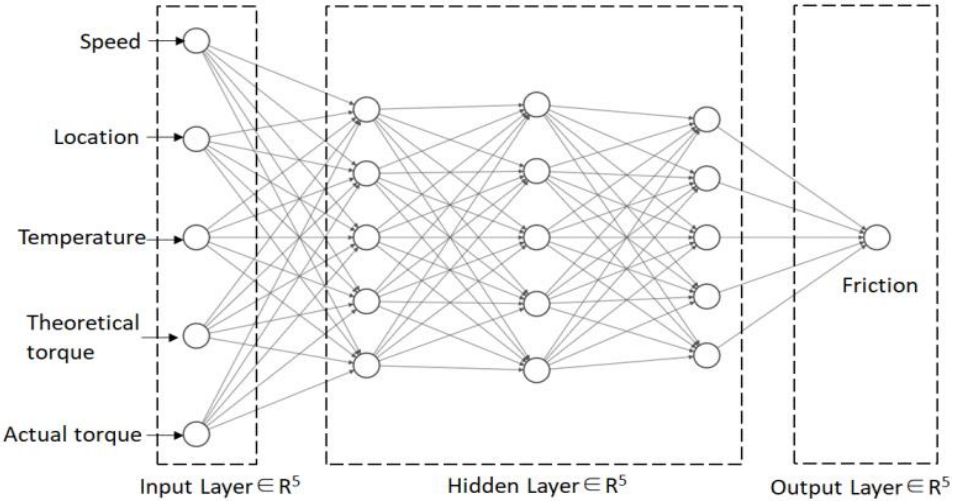

Fig. 4 Neural Network model

2.3 Data Preparation

2.3.1 Data Acquisition

The complex physical characteristics and mechanical structure inside the robot joints lead to frictional forces such as Coulomb friction, static friction, and viscous friction during the motion, and they have nonlinear characteristics. Usually, from the relative rest to the relative sliding between contact surfaces, according to the different main factors that determine the magnitude of friction, there are four stages [29], as shown in Fig. 5:

- I stage – the contact surface elastic deformation stage;
- II stage – the boundary lubrication stage;
- III stage – the partial liquid lubrication stage;
- IV stage – the whole liquid lubrication stage.

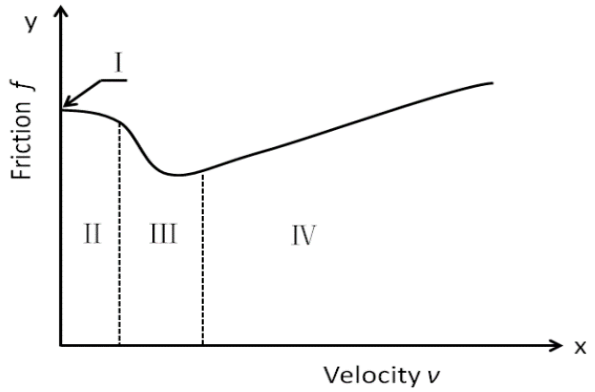

Fig. 5 Diagram of relationship between friction and velocity

Factors that affect the friction need to be considered in the sampling process:

1) When the robot joint moves, the instantaneous angular velocity change will cause the friction force magnitude to change accordingly.
2) The rotation of the robot joint at different positions causes the variation of the friction force, which is due to the other gaps inside its joints when the rotational axis of the robot joint is at different positions.
3) The motor and reducer of the target joint will cause micro-contact surface expansion, shrinkage and lubrication differences due to temperature changes. These factors make the friction change with temperature.
4) The pressure change caused by different radial loads of the target joint causes the friction force to change with the change of the axial load.
5) Different axial loads on the target joint lead to pressure variations, resulting in frictional force variations with axial load.
6) The mathematical relationship of "kinetic model (theoretical torque) + compensation model = measured torque".

Determination of the data collection scheme implies the following steps:

1) Acquisition of torque values at different speeds of wheel joints.
2) To collect the torque values of the wheel joints at different positions.
3) Collect torque values at different temperatures of wheel joints.
4) Based on the change of axle position, the torque data value is calculated according to the theoretical equation.
5) Using sensors to measure the actual torque and calibrate the torque accuracy of the servo system, etc.

The specific experimental approach was to program the mobile robot to specify eight different motion paths so that each joint axis of the robot moved at a different position and a different speed. The load, position, velocity, torque, and temperature of each joint of the mobile robot were recorded at sampling intervals of 4-10 ms during the eight sets of experiments. 29 sets of data were collected, including data for joints 1 to 4 of the robot, as shown in Table 2.

Table 2 Data collection

Collection data types	Number of data collected
Sampling time	1
Position planning value of each axis	4
Speed planning values for each axis	4
Theoretically calculated torque for each axis	4
Actual torque of each axis	4
Feedback position of each axis	4
Feedback speed per axis	4
Feedback torque of each axis	4

2.3.2 Data Processing

Before the model training, we perform the necessary processing on the collected data, mainly including data cleaning, classification, equalization, enhancement, etc. [30].

1) When data collection, as the path data of robot movement, may have the same group and missing data, data cleaning can ensure data integrity, uniqueness, and consistency.
2) Data classification is performed in advance according to the four states of acceleration, uniform speed, high speed, and low speed in robot motion, which facilitates the corresponding neural network model.
3) Because data acquisition cannot traverse all the motion data of robot conditions, data equalization can make model compensation more effective.
4) To improve the robustness of the model, data enhancements such as positive and negative transformations, translational transformations, and noise addition are utilized on the collected data, thus enhancing the generalization capability of the friction compensation model.

As the usage of the three different models implies training and testing of the models, in this work, 80% of the data collected render the training set, and 20% are the test set. In Fig. 6, the orange part is the test dataset, while the blue part is the training dataset.

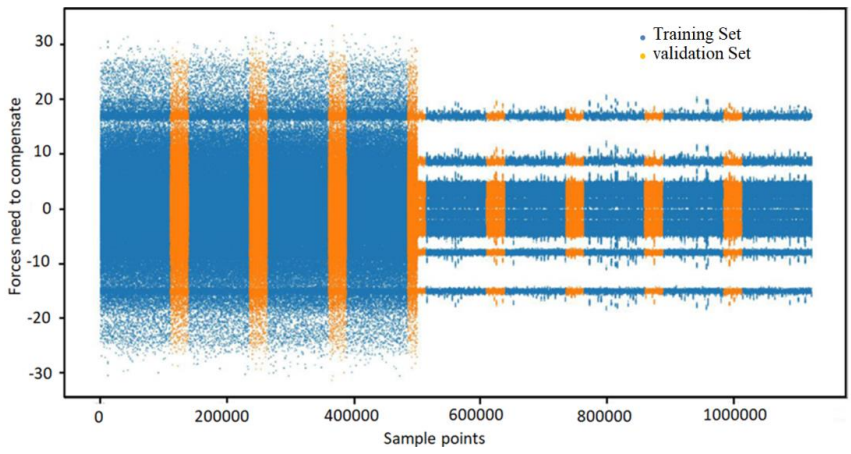

Fig. 6 Data set partitioning

3. EXPERIMENTS AND DISCUSSIONS

3.1 Model Training

This study uses two ways of dividing the data, and two different models are trained for each data division:

1) The first one is based on high or low speed and divided into low-speed and high-speed cases (with joint speed of 200 r/min as the boundary to distinguish between high and low speed).
2) The second is according to the acceleration speed rate and uniform speed case. (Because the acceleration and deceleration cases are similar, only the acceleration scenario is taken for analysis).

First, the data set used for initializing the neural network is prepared. In this study, the number of neurons in the input layer is 5. The number of neurons in the output layer is based on the solution to the problem, i.e., the friction of the robot joints and the neural network is trained using the five items: position, velocity, theoretical torque, actual torque, and temperature of the robot joints as the input to the neural network.

Second, the loss function when the neural network is defined during training. This study establishes the loss function as the following mathematical expression.

$$\text{loss} = \text{loss}\left(\mathrm{X}_i, \mathrm{Y}_i\right) = \left(\mathrm{X}_i - \mathrm{Y}_i\right)^2, \tag{9}$$

where, X_i is the neural network's practical output value, which is the forecast value, Y_i is the true value, i denotes the number of training data. Therefore, the training goal is to reduce the loss value as much as possible. Finally, there is the training of the neural network. The exact procedure of the training is as given in Fig. 7.

Step 1: Define the optimizer, select the optimization algorithm as well as the learning rate, pass all parameters of the neural network into the optimizer; define the loss function, which is the equation for calculating the error between the predicted and actual values of the neural network, and use Eq. (9) here.

Step 2: The training data is used as the input of the neural network. The training data, i.e., the position, speed, theoretical torque, actual torque, and temperature values of the robot joints, are used to obtain the corresponding output values through the neural network.

Step 3: The error between the output value of the neural network and the objective value, which is the value of the friction torque of the robot joint, is found according to the error calculation equation.

Step 4: Clear the residual update parameter values from the previous iteration.

Step 5: Error back propagation and calculation of updated parameter values.

Step 6: Make the parameter update values imposed on the parameters of the neural network.

Step 7: Determine if the present maximum iteration number is reached. If the current step number is less than the maximum iteration number, go to Step 2. If the current step number equals the maximum iteration step, then end.

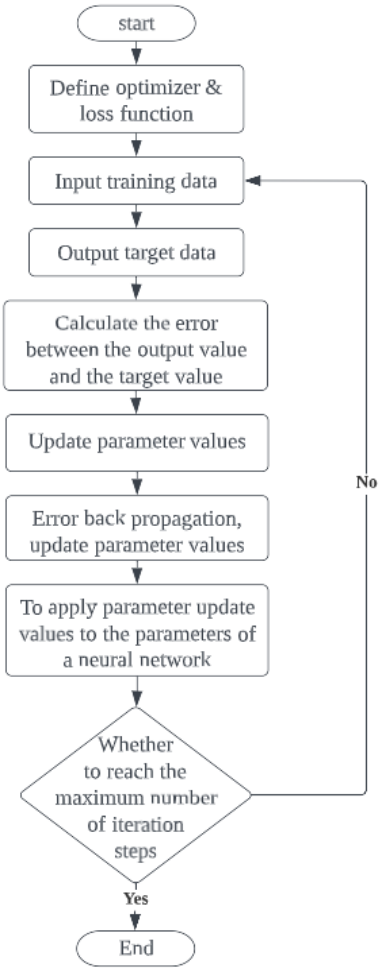

Fig. 7 Neural network training flow chart

In this study, the learning rate was set to 0.01, and the maximum number of iteration steps was set to 500 during training. The training tool uses the optimizer in PyTorch and the stochastic gradient descent algorithm SGD (Stochastic Gradient Descent) [31]. Since the stochastic gradient descent algorithm uses one sample in each iteration to update the parameters, the training is faster, and the specific mathematical expression for parameter update is as follows:

$$\theta_{j+1} = \theta_j + a\nabla_\theta loss \tag{10}$$

where a is the learning rate, θ_j is the weight coefficient under the *jth* iteration, j is the number of iterations, $\nabla_\theta loss$ is the gradient of the loss function.

When the number of iterative steps reaches 500, the loss value in the training process tends to zero, and the training ends. The final neural network fitting results (Figs. 8-11)

show that the output value of the neural network and the target value are the same for a given velocity of the robot joint, and the fitting effect is good.

Therefore, it is assumed that the initialized neural network has already learned the information about the correlation between the speed of the robot joints and the friction torque:

1) By low-speed and high-speed phases

- Low-speed phase

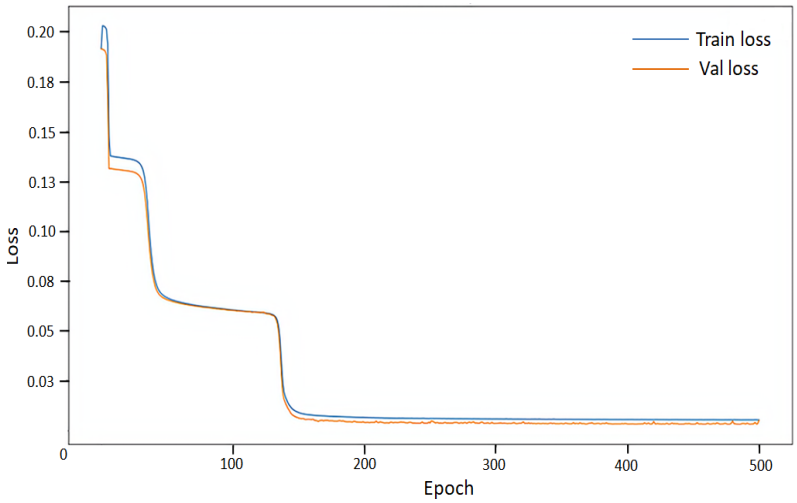

Fig. 8 Convergence diagram of low-speed stage

- High-speed phase

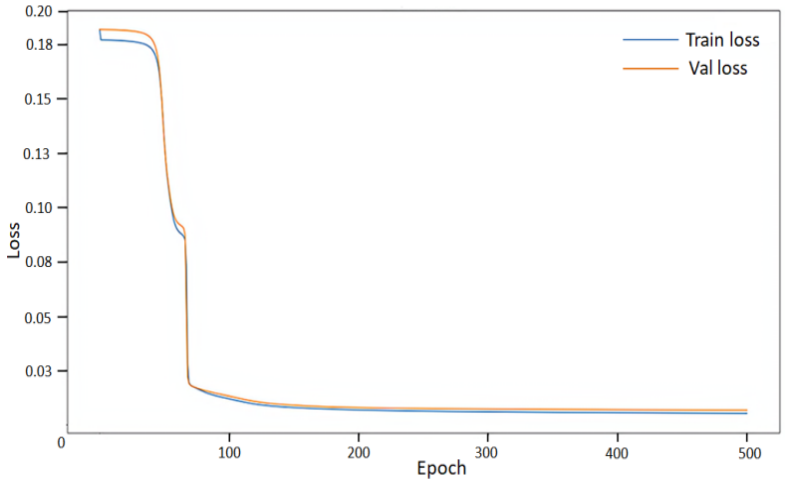

Fig. 9 Convergence diagram of high-speed stage

2) By Acceleration and uniform phase
- Acceleration phase:

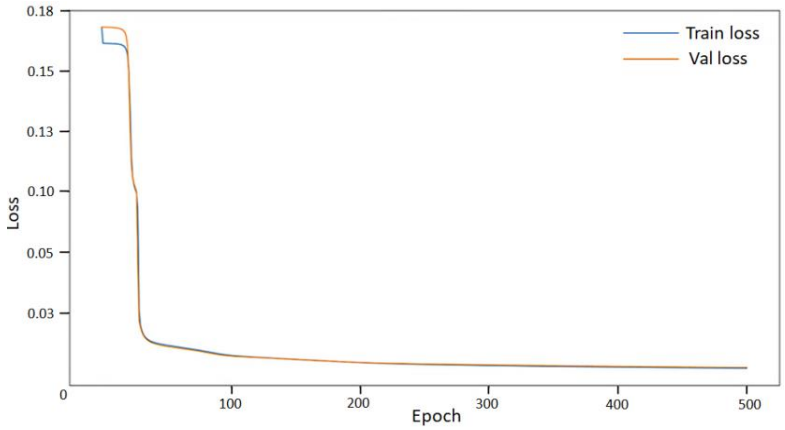

Fig. 10 Convergence diagram of the acceleration phase

- Uniform phase:

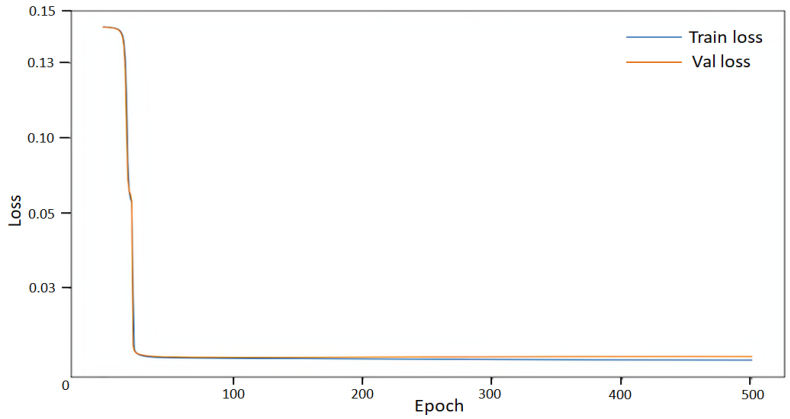

Fig. 11 Convergence diagram of uniform velocity stage

The conclusions are that the algorithm of the friction compensation model divided by acceleration/deceleration/homogeneous speed converged fastest, and the algorithm converged between 40-150 iterations. The algorithm converged fastest in the homogeneous speed condition and converged after 40 iterations because the friction force in the homogeneous speed condition was most stable. The algorithm converges slowest in the low-speed case, going through two convergence processes and converging after 150 iterations, which is due to the existence of multiple state transition processes for the friction inside the joint in the low-speed case, involving various stages such as elastic deformation stage, boundary lubrication stage, and partial liquid lubrication.

3.2 Training Results

The following shows the training effects of these three modes in four different scenarios: high speed, low speed, acceleration and uniform speed. The training results of the linear model are given in Fig 12.

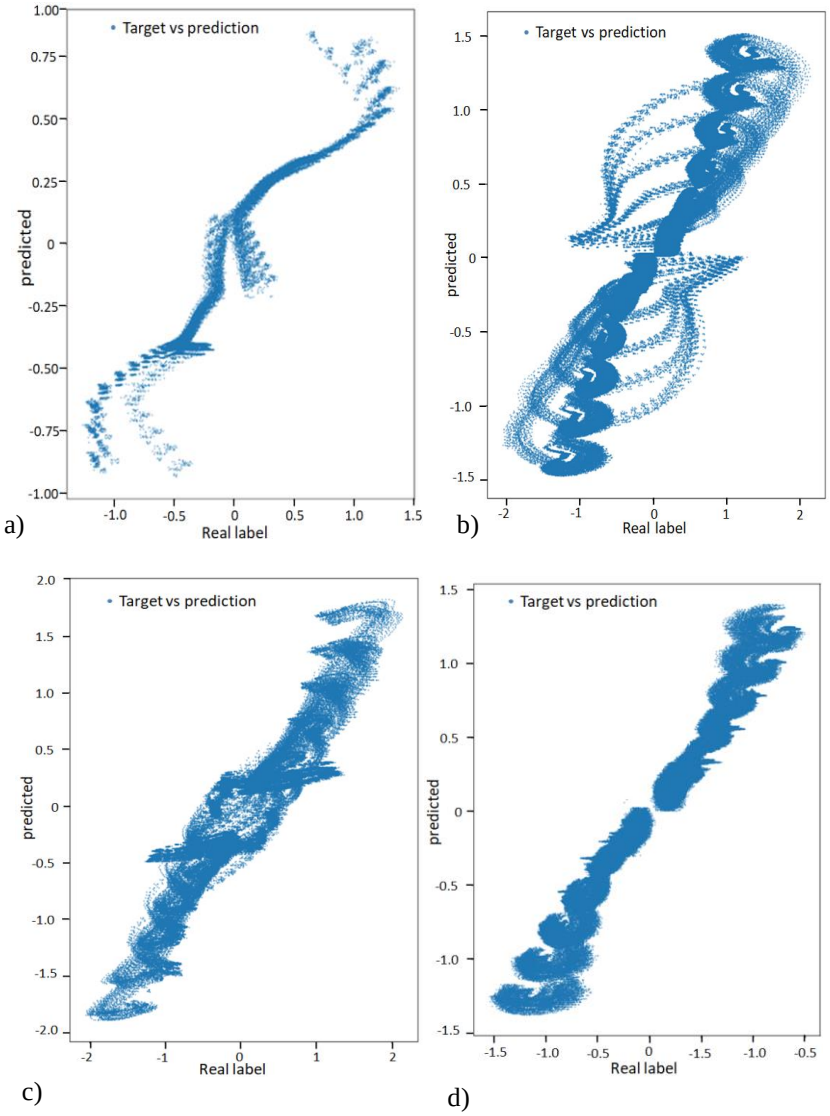

Fig. 12 Coefficient of determination curves tested using the linear model:
a) low-speed state, b) high-speed state, c) accelerated situation, d) uniform speed situation

The training results of the nonlinear model are presented in Fig. 13.

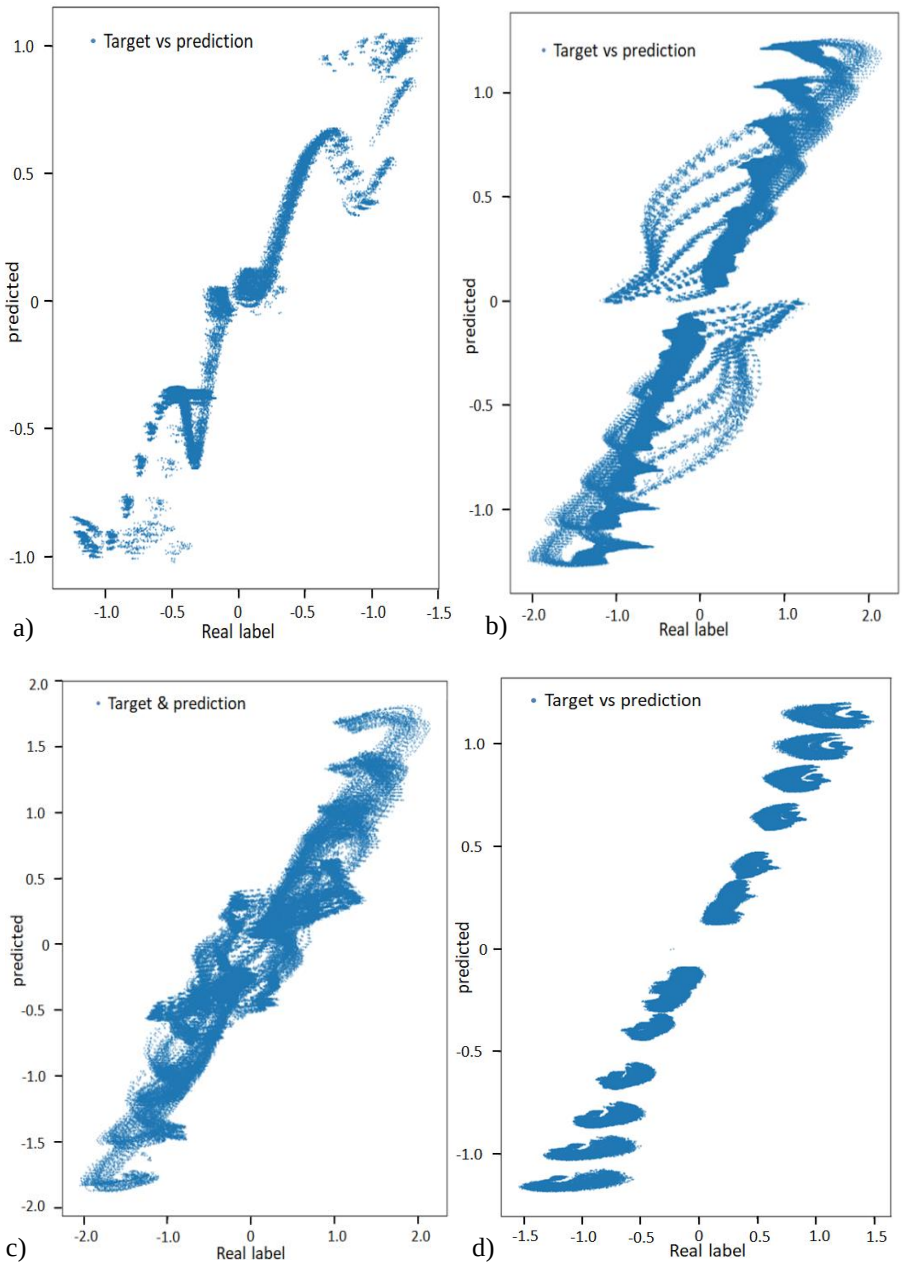

Fig. 13. Coefficient of determination curves tested using the nonlinear model: a) low-speed state, b) high-speed state, c) accelerated situation, d) uniform speed situation

Finally, the training results of the neural network model are depicted in Fig. 14.

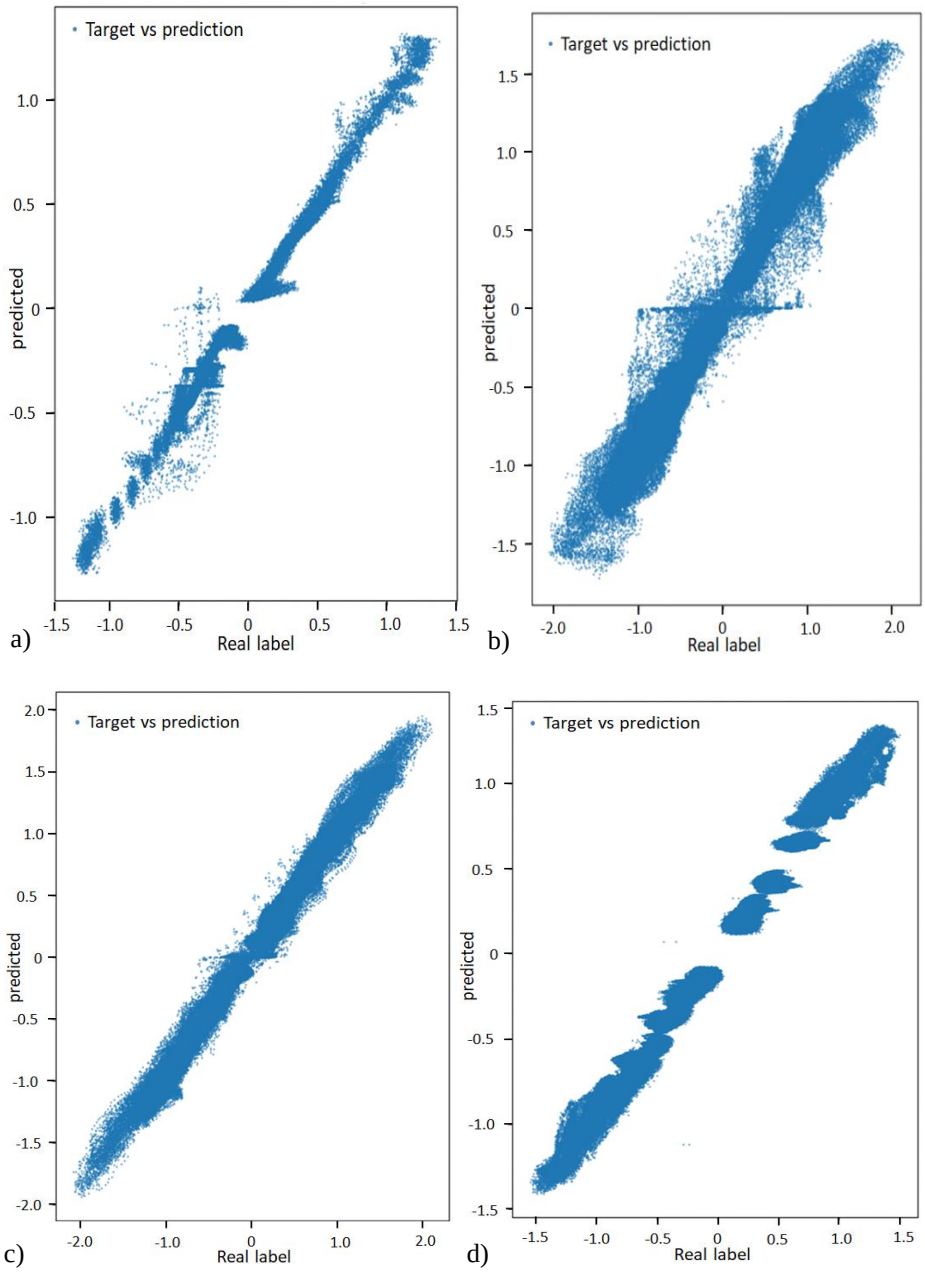

Fig. 14 Coefficient of determination curves tested using the Neural Network model: a) low-speed state, b) high-speed state, c) accelerated situation, d) uniform speed situation

The following conclusions are drawn from the results presented above:

- The learning results of neural networks are significantly better than other mathematical models.
- The model trained by the plus and uniform speed stage performs better in the test set than the model trained by the high and low speeds. Therefore, the combination of "neural network+training acceleration or homogeneous model" should be adopted to obtain the best friction compensation results.

3.3 Experimental validation

The experiment uses a four-wheeled mobile robot platform (Fig. 15) with a load capacity of 20 kg. The power unit drives four integrated joint modules by an industrial computer.

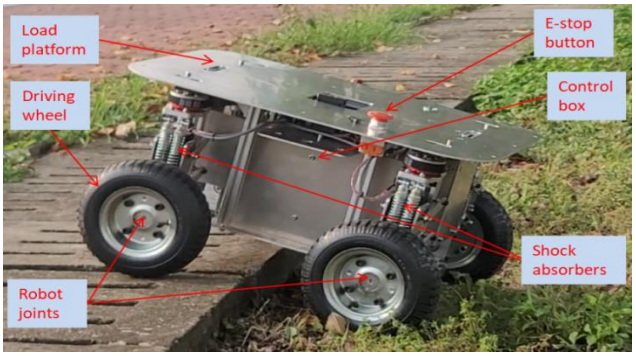

Fig. 15 Mobile robot test platform

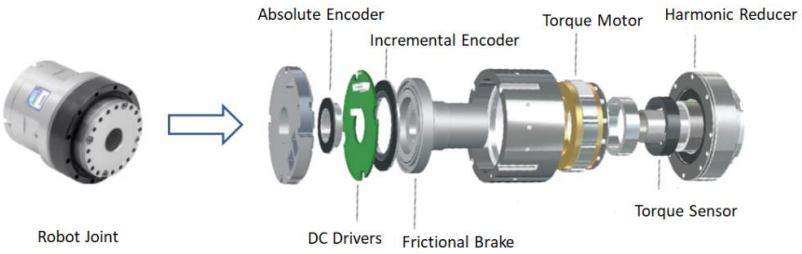

Fig. 16 Mobile robot's joint

Each integrated joint module (Fig. 16) comprises a harmonic reducer, frameless torque motor, brake, incremental encoder, absolute encoder, and servo driver, which is compact and easy to install. By comparing the position and speed of the feedback of the two encoders and referring to the drive current and motor torque output, the magnitude of the external force on the joint where the module is located can be determined.

The programming scheme is designed to test eight data sets in the practical application of mobile robots. The torque accuracy without friction compensation and with friction compensation is compared. The calculation method of torque relative error is Eq. 11.

$$\delta = \frac{\left(T_S + T_F - T_A\right)}{T_A} \times 100\% \tag{11}$$

Here, T_S is the theoretical torque, T_F is the frictional force compensation torque, T_A is the actual feedback torque.

In the calculation of the relative error, the data that are too small to cause the error explosion part of the original data have been excluded, where T_F is zero before friction compensation. The average relative error refers to the average of the relative error of each joint under different paths. It is given in Fig. 17.

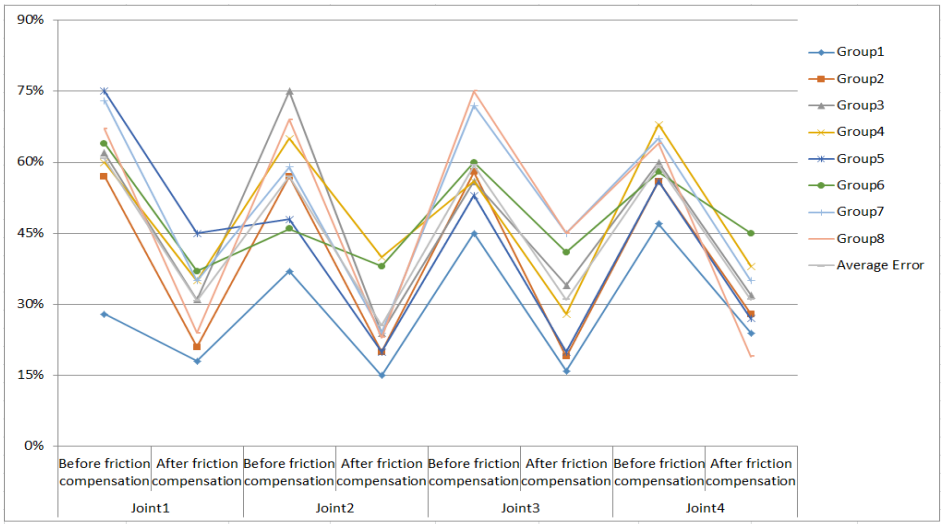

Fig. 17 Robot joint compensation error diagram

From the test data given in Table 3, it can be shown that the relative error δ of each joint of the mobile robot under eight test groups after friction compensation has been reduced to different degrees compared with that before compensation, and the values are concentrated in the range of 15% -75%.

Table 3 Friction compensation relative error table

Error (δ)	Joint 1		Joint 2		Joint 3		Joint 4	
	A	**B**	**A**	**B**	**A**	**B**	**A**	**B**
Group 1	28%	18%	37%	15%	45%	16%	47%	24%
Group 2	57%	21%	57%	20%	58%	19%	56%	28%
Group 3	62%	31%	75%	24%	56%	34%	60%	32%
Group 4	60%	35%	65%	40%	56%	28%	68%	38%
Group 5	75%	45%	48%	20%	53%	20%	56%	27%
Group 6	64%	37%	46%	38%	60%	41%	58%	45%
Group 7	73%	35%	59%	24%	72%	45%	65%	35%
Group 8	67%	24%	69%	23%	75%	45%	64%	19%
average error	61%	31%	57%	25.5%	59%	31%	59%	31%

*Note A is “Before friction compensation”; B is “after friction compensation”

4. CONCLUSIONS

In this study, to decrease the frictional force of mobile robot joints, we explore a suitable frictional force compensation model to give the robot joints the ability to adaptive adjust and improve accuracy. A friction compensation model based on deep learning is developed. The friction compensation model's inputs are load, position, speed, torque, and temperature data, and its outputs are friction compensation values. This deep learning-based robot joint friction recognition method can solve the problem that the existing friction model is not accurate and the recognition method is not precise enough. From the experimental results, the optimal friction compensation model is the "neural network + training acceleration and uniformity model", and this model can reduce the error best on the test set. By testing on the Four-wheel mobile robot experimental platform, the average relative error δ of each joint under different robot paths can reach 15% after friction compensation. This has practical significance for improving the accuracy of mobile robot joints. Future work will continue to explore the impact of the joint friction compensation model on mobile robot positioning accuracy.

REFERENCES

1. Kermani, M.R., Wong, M., Patel, R.V., Moallem, M., Ostojic, M., 2004, *Friction compensation in low and high-reversal-velocity manipulators*, IEEE International Conference on Robotics and Automation, Proceedings. ICRA'04, 5, pp. 4320-4325.
2. Iwatani, M., Kikuuwe, R., 2015, *An identification procedure for rate-dependent friction laws of robotic manipulator with limited motion range*, In 2015 10th Asian Control Conference (ASCC), pp. 1-5.
3. Marques, F., Flores, P., Pimenta Claro, J. C., Lankarani, H. M., 2016, *A survey and comparison of several friction force models for dynamic analysis of multibody mechanical systems*, Nonlinear Dynamics, 86, pp. 1407-1443.
4. Bona, B., Indri, M., 2005, *Friction compensation in robotics: an overview*, In Proceedings of the 44th IEEE Conference on Decision and Control, pp. 4360-4367.
5. Virgala, I., Frankovský, P., Kenderová, M., 2013, *Friction effect analysis of a DC motor*, American Journal of Mechanical Engineering, 1(1), pp. 1-5, doi: 10.12691/ajme-1-1-1
6. Richard, T., Germay, C., Detournay, E., 2007, *A simplified model to explore the root cause of stick–slip vibrations in drilling systems with drag bits*, Journal of sound and vibration, 305(3), pp. 432-456.
7. Nikfar, F., Konstantinidis, D., 2017, *Effect of the stick-slip phenomenon on the sliding response of objects subjected to pulse excitation*, Journal of Engineering Mechanics, 143(4), 04016122.
8. Keck, A., Zimmermann, J., Sawodny, O., 2017, *Friction parameter identification and compensation using the elastoplastic friction model*, Mechatronics, 47, pp. 168-182.
9. Beerens, R., Bisoffi, A., Zaccarian, L., Heemels, W. P., Nijmeijer, H., van de Wouw, N., 2018, *Hybrid PID control for transient performance improvement of motion systems with friction*, In 2018 Annual American Control Conference (ACC), pp. 539-544.
10. Wojtyra, M., 2017, *Modeling of static friction in closed-loop kinematic chains—Uniqueness and parametric sensitivity problems*, Multibody System Dynamics, 39(4), pp. 337-361.
11. Lampaert, V., Al-Bender, F., Swevers, J., 2003, *A generalized Maxwell-slip friction model appropriate for control purposes*, In 2003 IEEE International Workshop on Workload Characterization, 4, pp. 1170-1177.
12. Xu, L., Yao, B., 2008, *Adaptive robust control of mechanical systems with non-linear dynamic friction compensation*, International Journal of control, 81(2), pp. 167-176.
13. Piasek, J., Patelski, R., Pazderski, D., Kozłowski, K., 2019, *Identification of a dynamic friction model and its application in a precise tracking control*, Acta Polytechnica Hungarica, 16(10), pp. 83-99.
14. Swevers, J., Al-Bender, F., Ganseman, C.G., Projogo, T., 2000, *An integrated friction model structure with improved presliding behavior for accurate friction compensation*, IEEE Transactions on automatic control, 45(4), pp. 675-686.
15. Lee, T.H., Tan, K.K., Huang, S., 2010, *Adaptive friction compensation with a dynamical friction model*, IEEE/ASME transactions on mechatronics, 16(1), pp. 133-140.
16. Iskandar, M., Wolf, S., 2019, *Dynamic friction model with thermal and load dependency: modeling, compensation, and external force estimation*, In 2019 International Conference on Robotics and Automation (ICRA), pp. 7367-7373.

17. Piasek, J., Patelski, R., Pazderski, D., Kozłowski, K., 2019, *Identification of a dynamic friction model and its application in a precise tracking control*, Acta Polytechnica Hungarica, 16(10), pp. 83-99.
18. Gandarilla, I., Santibáñez, V., Sandoval, J., Campa, R., 2022, *Joint position regulation of a class of underactuated mechanical systems affected by LuGre dynamic friction via the IDA-PBC method*, International Journal of Control, 95(6), pp. 1419-1431.
19. Cılız, M.K., Tomizuka, M., 2007, *Friction modelling and compensation for motion control using hybrid neural network models*, Engineering Applications of Artificial Intelligence, 20(7), pp. 898-911.
20. Doan, Q.V., Le, T.D., Le, Q.D., Kang, H.J., 2018, *A neural network–based synchronized computed torque controller for three degree-of-freedom planar parallel manipulators with uncertainties compensation*, International Journal of Advanced Robotic Systems, 15(2), doi: 10.1177/1729881418767307.
21. Grami, S., Okonkwo, P.C., 2021, *Friction Compensation in Robot Manipulator Using Artificial Neural Network*, In Advances in Automation, Signal Processing, Instrumentation, and Control: Select Proceedings of i-CASIC 2020, pp. 641-650.
22. Yen, V.T., Nan, W.Y., Van Cuong, P., Quynh, N.X., Thich, V.H., 2017, *Robust adaptive sliding mode control for industrial robot manipulator using fuzzy wavelet neural networks*, International Journal of Control, Automation and Systems, 15(6), pp. 2930-2941.
23. Ali, K., Ullah, S., Mehmood, A., Mostafa, H., Marey, M., Iqbal, J., 2022, *Adaptive FIT-SMC approach for an anthropomorphic manipulator with robust exact differentiator and neural network-based friction compensation*, IEEE Access, 10, pp. 3378-3389.
24. Ruan, W., Dong, Q., Zhang, X., Li, Z., 2021, *Friction compensation control of electromechanical actuator based on neural network adaptive sliding mode*, Sensors, 21(4), 1508.
25. Nevmerzhitskiy, M.N., Notkin, B.S., Vara, A.V., Zmeu, K.V., 2019, *Friction model of industrial robot joint with temperature correction by example of KUKA KR10*, Journal of Robotics, 2019, 6931563.
26. Bittencourt, A.C., Wernholt, E., Sander-Tavallaey, S., Brogårdh, T., 2010, *An extended friction model to capture load and temperature effects in robot joints*, Proceedings of 2010 IEEE/RSJ international conference on intelligent robots and systems, pp. 6161-6167.
27. Raviola, A., Guida, R., De Martin, A., Pastorelli, S., Mauro, S., Sorli, M., 2021, *Effects of temperature and mounting configuration on the dynamic parameters identification of industrial robots*, Robotics, 10(3), 83.
28. Thomas, A.J., Petridis, M., Walters, S.D., Gheytassi, S.M., Morgan, R. E., 2017, *Two hidden layers are usually better than one*, In Engineering Applications of Neural Networks: 18th International Conference, EANN 2017, Athens, Greece, Proceedings, pp. 279-290.
29. Xu, H., Shi, Z., Yu, B., Wang, H., 2019, *Optimal measurement speed and its determination method in the transmission precision evaluation of precision reducers*, Applied Sciences, 9(10), 2146.
30. Maharana, K., Mondal, S., Nemade, B., 2022, *A review: Data pre-processing and data augmentation techniques*, Global Transitions Proceedings, 3(1), pp. 91-99.
31. Gower, R.M., Loizou, N., Qian, X., Sailanbayev, A., Shulgin, E., Richtárik, P., 2019, *SGD: General analysis and improved rates,* In International conference on machine learning, pp. 5200-5209.